Liquid-vapor transition of systems with mean field universality class

Gernot J. Pauschenwein[a)]
CMS and Institut für Theoretische Physik, TU Wien, Wiedner Hauptstraße 8-10, A-1040 Wien, Austria

Jean-Michel Caillol,[b)] Dominique Levesque,[c)] and Jean-Jacques Weis[d)]
Laboratoire de Physique Théorique, UMR 8627, Université Paris-Sud, Bâtiment 210, 91405 Orsay Cedex, France

Elisabeth Schöll-Paschinger[e)]
CMS and Fakultät für Physik, Universität Wien, Boltzmanngasse 5, A-1090 Wien, Austria

Gerhard Kahl[f)]
CMS and Institut für Theoretische Physik, TU Wien, Wiedner Hauptstraße 8-10, A-1040 Wien, Austria

We have considered a system where the interaction, $v(r) = v_{IS}(r) + \xi^2 v_{MF}(r)$, is given as a linear combination of two potentials, each of which being characterized with a well-defined critical behavior: for $v_{IS}(r)$ we have chosen the potential of the restricted primitive model which is known to belong to the three-dimensional Ising universality class, while for $v_{MF}(r)$ we have considered a long-range interaction in the Kac [J. Math. Phys. **4**, 216 (1963)] limit, displaying mean field (MF) behavior. We study the performance of two theoretical approaches and of computer simulations in the critical region for this particular system and give a detailed comparison between theories and simulation of the critical region and the location of the critical point. Having shown by theoretical arguments that the system belongs to the MF universality class for any positive value of ξ and shows nonclassical behavior only for $\xi = 0$, we examine to which extent theoretical approximations and simulation can reproduce this behavior. While in this limiting case theoretical approaches are known to fail, we find good agreement for the critical properties between the theoretical approaches and the simulations for ξ^2 larger than 0.05. © *2007 American Institute of Physics*.
[DOI: 10.1063/1.2405353]

I. INTRODUCTION

The exact determination of the critical properties of a fluid (i.e., in terms of the location of its critical point and of its universality class) represents a formidable challenge both to theoretical approaches as well as to computer simulations. Although integral-equation theories are quite successful in predicting the thermodynamic and structural properties of a variety of simple and more complex systems over a wide domain in temperature-density space,[1] they meet with variable success in the critical region due to an unsatisfactory treatment of long wavelength fluctuations which are of particular relevance in this region.[2,3] To give an example, for the modified hypernetted chain equation (MHNC), which is amongst the most accurate liquid state theories,[4] the boundary of the density region at which no solution is found does not correspond to the spinodal and there is no divergence of the compressibility. The mean spherical approximation (MSA), on the other hand, satisfies scaling laws in the critical region, though with peculiar critical exponents (mean spherical exponents[5]), but, similar to MHNC, fails to give a

proper treatment of the first order gas-liquid (GL) transition.[2] For computer simulations, on the other hand, suitable techniques have been developed that allow the determination of the critical point via data extrapolation from simulations performed in finite simulation volumes.[6–8]

The purpose of the present paper is to examine the performance of theoretical approaches and of computer simulations in the critical region for a system where the potential $v(r)$ is a linear combination of two interactions, exhibiting different, but well-established critical behavior, i.e., three-dimensional (3D) Ising (IS) and mean field (MF),

$$v(r) = v_{IS}(r) + \xi^2 v_{MF}(r). \tag{1}$$

The dimensionless parameter ξ^2 indicates the relative importance of the two contributions. For reasons given below, we shall use a Coulombic interaction for $v_{IS}(r)$ and a Kac potential[9,10] for $v_{MF}(r)$ which we define as the limit, at fixed volume V,

$$v_{MF}(r) = \lim_{\alpha^* \to 0} \alpha^{*3} \Phi(\alpha^* x), \tag{2}$$

where $\Phi(x) = -(q^2/\sigma)(e^{-x}/x)$ ($x = r/\sigma$, σ length scale, and q has the dimension of a charge). When the dimensionless parameter $\alpha^* = \alpha\sigma$ tends to zero the strength of the potential decreases and its range increases to infinity. It is crucial to observe that the limit $\alpha \to 0$ in Eq. (2) must be taken *before* taking the thermodynamic limit, i.e., at fixed volume. Al-

a)Electronic mail: pauschenwein@cmt.tuwien.ac.at
b)Electronic mail: jean-michel.caillol@th.u-psud.fr
c)Electronic mail: dominique.levesque@th.u-psud.fr
d)Electronic mail: jean-jacques.weis@th.u-psud.fr
e)Electronic mail: elisabeth.schoell-paschinger@univie.ac.at
f)Electronic mail: gkahl@tph.tuwien.ac.at

though one might expect that the critical behavior of the system is the result of a competition between the Ising 3D and the MF behavior, leading, for example, to a crossover between the two universality classes, it turns out that the criticality of the system is described by a MF behavior except at $\xi^2=0$ where the system behaves Ising-3D-like.

To overcome the problem of liquid state theories mentioned above, two advanced liquid state theories have been proposed in recent years that are able to provide accurate data in the critical region: the hierarchical reference theory (HRT) of Parola and Reatto[3] and the self-consistent Ornstein-Zernike approximation (SCOZA) originally proposed by Høye and Stell.[11,12] Compared to standard liquid state theories they are more successful in describing the critical region, providing, in particular, nonclassical (i.e., non-MF) critical exponents. The HRT approach is a successful merger[2,3] of liquid state theory with renormalization group ideas. In the simplest form of SCOZA (Refs. [13–15]) (which will be used here) the Ornstein-Zernike (OZ) equation is supplemented by an approximate, MSA-type closure relation for the direct correlation function containing a density- and temperature-dependent function which is determined by imposing self-consistency between the compressibility and internal energy routes to the thermodynamics. SCOZA predicts non-MF critical exponents;[16] they are different when approaching the critical temperature from above or below and, in both cases, satisfy hyperscaling.[16] We note that the formalism of SCOZA is not applicable for the Kac potential (i.e., for $\alpha=0$) itself; instead, we rather have to consider a potential with a small, but finite parameter α. On the other hand, this restriction also has the attractive feature that we can study in detail how the critical behavior varies as α tends to zero; indeed we can identify a crossover behavior between a nonclassical and a MF behavior.

In addition we use a recent improved mean field theory based on a loop expansion of the free energy of the restrictive primitive model[17,18] (RPM) to describe the thermodynamic properties of our system.

Finally, we have used grand canonical Monte Carlo (GCMC) simulations performed on a hypersphere[19,20] together with histogram reweighting techniques[21] to locate the critical point and the near critical coexistence curve.[6,22]

With respect to the contribution to $v(r)$ with Ising 3D criticality we resorted to the RPM. This choice has three advantages: first, it is now well established by simulations that the RPM belongs to the Ising 3D universality class.[23,24] In addition, the critical parameters (i.e., temperature T_c and density ρ_c) and the near critical coexistence curve are accurately known. Second, the reduced, dimensionless, critical temperature and density of the RPM, $T_c \approx 0.0489-0.0492$, $\rho_c \approx 0.076-0.080$ (Refs. [23–25]) (for the definition of the reduced units see Sec. II) differ notably from those of the Kac model $(\lim_{\xi^2 \to \infty} T_c/\xi^2 \approx 1.130\,52,\ \rho_c \approx 0.27)$, which would not be the case by taking for $v_{IS}(r)$ a short range Yukawa potential. Third, the improved MF theory outlined above can be formulated with closed expressions for a size-symmetric (and possibly charge-asymmetric) system of charged hard spheres, including thus the RPM.[17] These attractive features are contrasted by one serious disadvantage: theoretical ap-

proaches that have been proposed up to date in the literature are not able to provide results for T_c and ρ_c for the RPM that are in reasonable agreement with the predictions of simulation.[17,26–28] Nevertheless, the critical exponents we obtain from our SCOZA investigation for the RPM show a crossover behavior to MF.

The paper is organized as follows. After presenting our model (Sec. II), we give a brief introduction to the theoretical concepts that we apply to study the critical behavior of our system: an improved MF theory and SCOZA (Sec. III). The section is closed with a comparison between the data produced by these concepts. In Sec. IV we give details about the simulation techniques that we apply and discuss the problems hereby encountered. In the subsequent section (Sec. V) we make a comparison between the data obtained in the theoretical approaches and in the simulations. The paper is closed with concluding remarks.

II. MODEL AND REDUCED UNITS

Using the RPM for $v_{IS}(r)$, our potential $v(r)$ is actually the interaction of a binary system, thus

$$v_{ij}(r) = \begin{cases} \infty, & r \le \sigma \\ \dfrac{q_i q_j}{r} + \xi^2 v_{MF}(r), & r > \sigma, \end{cases} \quad (3)$$

where $v_{MF}(r)$ is given in Eq. (2).

Numerical results will be expressed in reduced units [taking the hard-sphere (HS) diameter σ as unit of length]: reduced temperature $T^* = 1/\beta^*$, where $\beta^* = q^2/k_B T \sigma$ ($q = q_+ = -q_-$ charge of the spheres, k_B Boltzmann constant, and T temperature), reduced configurational chemical potential $\mu^* = \mu/k_B T$, reduced volume $V^* = V/\sigma^3$, and reduced density $\rho^* = N/V^*$ (N the number of particles). However, for notational convenience we will drop the stars throughout the paper.

III. THEORY

A. Improved mean field theory (MF2L)

The Kac potential energy $E_p(\mathcal{C})$ of a grand canonical (GC) configuration $\mathcal{C}$, assuming, for instance, periodic boundary conditions, is

$$E_p(\mathcal{C}) = \frac{1}{2V} \sum_{k \in \Lambda} \tilde{v}_{MF}(k) \tilde{\rho}(k) \tilde{\rho}(-k), \quad (4)$$

where $\tilde{v}_{MF}(k)$ and $\tilde{\rho}(k)$ are the Fourier transforms of $v_{MF}(r)$ and the microscopic density, respectively. For a fixed volume V, $\tilde{v}_{MF}(k) = \tilde{\Phi}(k/\alpha)$ vanishes for all nonzero $(k \ne 0)$ wave vectors of Fourier space in the limit $\alpha \to 0$ and $\tilde{v}_{MF}(0) = \tilde{\Phi}(0)$. Thus

$$E_p(\mathcal{C}) = \frac{1}{2V} \tilde{\rho}(0)^2 \tilde{\Phi}(0) = -2\pi q^2 V \rho^2. \quad (5)$$

The GC partition function of the model [Eq. (1)] is then obtained as[18]

$$\Xi_V(\beta,\nu) \simeq \int_0^\infty d\rho\sigma^3$$

$$\times \exp[-V(-\nu\rho + \beta f_{RPM}(\rho) - 2\pi\beta q^2\xi^2\rho^2)], \tag{6}$$

where we have replaced the sum over the number of particles by an integral over the density which is valid for large systems and has no consequences for the thermodynamic limit (here $\beta = 1/k_B T$). In Eq. (6), $f_{RPM}(\rho,\beta)$ is the Helmholtz free energy per unit volume of the RPM fluid at density ρ and $\nu \equiv \beta\mu$. Taking now the limit $V \to \infty$, one gets

$$\lim_{V\to\infty} -\frac{1}{V}\ln\Xi_V(\beta,\nu) = \min_\rho \mathcal{L}(\beta,\nu,\rho),$$

$$\mathcal{L}(\beta,\nu,\rho) = -\nu\rho + \beta f_{RPM}(\rho,\beta) - 2\pi\beta q^2\xi^2\rho^2. \tag{7}$$

The function $\mathcal{L}(\beta,\nu,\rho)$ plays the role of a Landau function.[18,29] Denoting β_c^{RPM} the inverse critical temperature of the RPM, we note that $\beta f_{RPM}(\rho,\beta)$ is an analytical and *strictly* convex function of ρ for $\beta < \beta_c^{RPM}$. Therefore, since the critical point of our model (cf. the simulation results of Sec. V) occurs for $\beta < \beta_c^{RPM}$, the analyticity of $f_{RPM}(\rho,\beta)$ for these temperatures obviously implies that in the vicinity of the critical point the derivatives with respect to ρ and β and the Taylor expansion of $\mathcal{L}(\beta,\nu,\rho)$ are well-defined quantities. From the standard analysis made in Ref. 47 and the analysis of the Kac model, it can thus be inferred that the composite system [Eq. (1)] will have MF behavior.[9,18]

Equation (7) can be taken as the starting point for an improved MF theory. To this end an approximate expression for $f_{RPM}(\beta,\rho)$ is inserted in the Landau function $\mathcal{L}(\beta,\nu,\rho)$ of Eq. (7) and $\mathcal{L}(\beta,\nu,\rho)$ minimized with respect to ρ for each inverse temperature β and reduced chemical potential ν. At low temperatures and arbitrary ν, $\mathcal{L}(\beta,\nu,\rho)$ has in general two minima, ρ_g and ρ_l, but there is only one value of ν, i.e., $\nu_{coex}(\beta)$, for which the Landau function takes equal values at the two minima. The corresponding minima are the densities of the gas and liquid phases at coexistence, respectively.

We have used for f_{RPM} the loop expansion of the RPM free energy obtained in the field theoretical framework of Refs. 17 and 18, i.e.,

$$f_{RPM} = f_{RPM}^{(0)} + f_{RPM}^{(1)} + f_{RPM}^{(2)} + \cdots, \tag{8}$$

where the superscripts (p) denote the pth order contribution to the loop expansion of f_{RPM}.

At the tree level one has for the RPM,[17]

$$\beta f_{RPM}^{(0)} = \beta f_{HS}(\rho) - \rho\ln 2 - \frac{\rho}{2}\beta q^2 v_c(0), \tag{9}$$

where $f_{HS}(\rho)$ denotes the excess free energy per unit volume of the reference HS fluid for which the Carnahan-Starling approximation[30] was used in numerical calculations. The $\rho\ln 2$ contribution stems from the entropy of mixing and $v_c(r)$ denotes the Coulomb potential, $v_c(r) = 1/r$ for $r > \sigma$ and regularized inside the core region.

The one-loop contribution $\beta f_{RPM}^{(1)}$ reads

$$\beta f_{RPM}^{(1)} = \frac{1}{2}\int \frac{d^3\mathbf{k}}{(2\pi)^3}\ln[1 + \beta\rho q^2\tilde{v}_c(k)] \tag{10}$$

and coincides with the free energy in the random phase approximation (RPA).[17]

Finally, the two-loop contribution $\beta f_{RPM}^{(2)}$, still tractable, has the expression

$$\beta f_{RPM}^{(2)} = -\frac{\beta^2}{4}[\rho q^2]^2 \int d^3\mathbf{r} h_{HS,\rho}(r)\Delta^2(r), \tag{11}$$

where $h_{HS,\rho}(r)$ denotes the usual pair distribution function of HSs at number density ρ; $\Delta(r)$ the propagator of the free theory whose expression in k space is[17]

$$\tilde{\Delta}(k) = \frac{\tilde{v}_c(k)}{1 + \beta\rho q^2\tilde{v}_c(k)}. \tag{12}$$

As discussed at length in Refs. 17 and 18 the loop expansion is not a systematic expansion in some small physical parameter and thus depends explicitly on the regularization of the Coulomb potential $v_c(r)$ in the core ($r < \sigma$). In this work we adopted the MSA regularization[17] which ensures that, at the one-loop level, the pair distribution function vanishes inside the core. Moreover, with this specification the one-loop approximation of f_{RPM} coincides with the optimized RPA theory or the MSA theory if one adopts, as we did, the Percus-Yevick expression[4] for $h_{HS,\rho}(r)$.

With the MSA regularization,[4]

$$v_{c,MSA}(r) = 1/r \quad (r \geq \sigma), \tag{13}$$

$$v_{c,MSA}(r) = \frac{B}{\sigma}\left(2 - \frac{Br}{\sigma}\right) \quad (0 \leq r \leq \sigma), \tag{14}$$

$$B = \frac{x^2 + x - x(1+2x)^{1/2}}{x^2}, \tag{15}$$

where $x = \kappa\sigma$ and $\kappa^2 = 4\pi\beta\rho q^2$ is the Debye wave number squared.

B. SCOZA

As noted in the Introduction the formalism of SCOZA is not applicable if we choose in our interaction $v_{ij}(r)$ α to be zero. Therefore we consider a slightly modified potential, $\bar{v}_{ij}(r)$, the so-called charged Yukawa model,[31]

$$\bar{v}_{ij}(r) = v_{ij}^C(r) + \xi^2 v^Y(r), \quad i,j = +,-, \tag{16}$$

where $v_{ij}^C(r)$ stands again for the RPM, while the Yukawa (Y) contribution reads

$$v^Y(r) = \begin{cases} \infty, & r \leq \sigma \\ -q^2\dfrac{\alpha^{*2}}{r}e^{-\alpha^* r/\sigma}, & r > \sigma. \end{cases} \tag{17}$$

In the limit $\alpha^* \to 0$, $v^Y(r)$ reduces to $v_{MF}(r)$.

For this particular system the set of OZ equations,

$$h_{ij}(r) = c_{ij}(r) + \sum_k \rho_k [h_{ik} \otimes c_{kj}](r), \quad i,j,k = +,-, \quad (18)$$

where "$\otimes$" denotes the convolution operation, can be decoupled: with $\rho_- = \rho_+ = \rho/2$ and $q_+ = -q_- = q$ and introducing the correlation functions

$$h^Y(r) = \tfrac{1}{2}[h_{++}(r) + h_{+-}(r)], \quad c^Y(r) = \tfrac{1}{2}[c_{++}(r) + c_{+-}(r)], \quad (19)$$

$$h^C(r) = \tfrac{1}{2}[h_{++}(r) - h_{+-}(r)], \quad c^C(r) = \tfrac{1}{2}[c_{++}(r) - c_{+-}(r)], \quad (20)$$

the set of OZ equations (18) decomposes into two independently solvable one-component OZ equations for the Yukawa and the Coulomb parts, namely,

$$h^Y(r) = c^Y(r) + \rho[h^Y \otimes c^Y](r),$$
$$h^C(r) = c^C(r) + \rho[h^C \otimes c^C](r). \quad (21)$$

The formalism of SCOZA (Refs. 13 and 32) is based on the MSA closure to the OZ equations, i.e.,

$$g_{ij}(r) = 0 \quad \text{for } r \leq \sigma,$$
$$c_{ij}(r) = -\beta \bar{v}_{ij}(r) \quad \text{for } r > \sigma. \quad (22)$$

Introducing $g^Y(r) = h^Y(r) + 1$ and $g^C(r) = h^C(r)$ leads to the MSA closure for the decoupled OZ equations (21),

$$h^Y(r) = -1, \quad r \leq \sigma,$$
$$c^Y(r) = c^{HS}(r) - \beta v^Y(r), \quad r > \sigma, \quad (23)$$

and

$$h^C(r) = 0, \quad r \leq \sigma,$$
$$c^C(r) = -\beta \frac{q^2}{r}, \quad r > \sigma. \quad (24)$$

Above we have used for the correlation function of the HS reference system, $c^{HS}(r)$, the Waisman parametrization (for details see Ref. 33),

$$c^{HS}(r) = K_1(\rho) \frac{\exp[-z_1(\rho)(r - \sigma)]}{r}. \quad (25)$$

For the Yukawa part the formalism of SCOZA can be applied in a straightforward way; introducing a yet unknown, state-dependent function $K^Y(\rho, T)$, the SCOZA closure relation (23) reads

$$h^Y(r) = -1, \quad r \leq \sigma,$$
$$c^Y(r) = c^{HS}(r) - K^Y(\rho, T) v^Y(r), \quad r > \sigma. \quad (26)$$

For the Coulomb part the situation is more delicate: in Coulomb systems the Stillinger-Lovett sum rules[4,34] have to be satisfied which would be violated when introducing a function $K^C(\rho, T)$, similar to what we did for the Yukawa contribution in Eq. (26). We therefore cannot extend SCOZA to the Coulomb part and have to treat it rather within MSA, i.e., we use the closure relations (24) for $h^C(r)$ and $c^C(r)$.

Within the SCOZA formalism a partial differential equation (PDE) is derived that imposes thermodynamic self-consistency between the energy and compressibility routes and thus fixes the yet undetermined function $K^Y(\rho, T)$. Thus we have to calculate the internal energy and the compressibility of the system within the framework of our theory. A straightforward analysis leads to

$$u = \frac{u^{\text{ex}}}{V} = 2\pi \sum_{i,j=+,-} \rho_i \rho_j \int dr\, r^2 g_{ij}(r) \bar{v}_{ij}(r) = u^Y + u^C, \quad (27)$$

with u^{ex} being the excess (over HS) internal energy and introducing

$$u^Y = 2\pi\rho^2 \int dr\, r^2 g^Y(r) v^Y(r) \quad (28)$$

and

$$\beta u^C = 2\pi\rho^2 \beta \int_0^\infty g^C(r) q^2 r\, dr$$
$$= \frac{w}{4\pi\sigma^3}(\sqrt{1+2w} - 1 - w),$$
$$w = \sqrt{\frac{4\pi\rho\sigma^2 q^2}{k_B T}}. \quad (29)$$

The explicit expression of u^C was derived within MSA by Waisman and Lebowitz.[35]

In a similar manner the reduced, dimensionless compressibility $\chi_{\text{red}}(=\rho k_B T \chi_T)$ can be calculated for our system, leading to

$$(\chi_{\text{red}})^{-1} = 1 - \frac{\rho}{2}[\tilde{c}_{++}(0) + \tilde{c}_{+-}(0)] = 1 - \rho\tilde{c}^Y(0), \quad (30)$$

where the tilde denotes the Fourier transform.

SCOZA imposes thermodynamic consistency between the energy and the compressibility routes via the following PDE:

$$\rho \frac{\partial^2 u}{\partial \rho^2} = \frac{\partial}{\partial \beta}\left(\frac{1}{\chi_{\text{red}}}\right). \quad (31)$$

Using Eqs. (27)–(30) and a few trivial manipulations one ends up with the following equation:

$$B(\rho, u^Y)\frac{\partial u^Y}{\partial \beta} + D(\rho, u^C) = C(\rho)\frac{\partial^2 u^Y}{\partial \rho^2}, \quad (32)$$

i.e., a PDE which has a structure similar to the standard SCOZA-PDE for the one-component fluid (see, e.g., Ref. 15). $B(\rho, u^Y)$ is formally identical to the corresponding standard SCOZA expression[36] $B(\rho, u)$ and is obtained for the present problem by simply replacing u by u^Y; again, $C(\rho) = \rho$. Finally, one finds for the additional coefficient $D(\rho, u^C)$ the following relation:
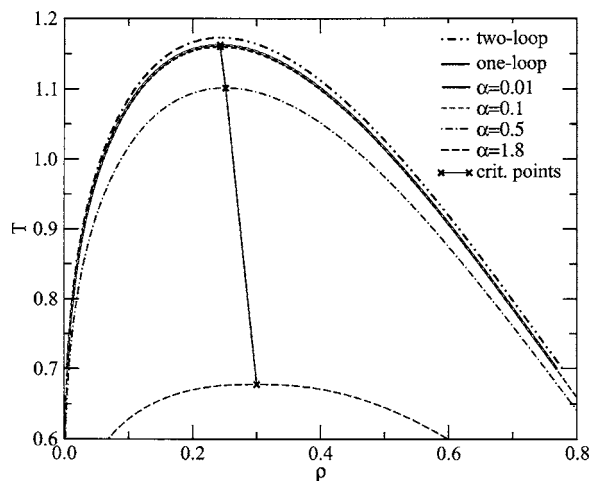
FIG. 1. Phase diagram in the (T, ρ) plane of the system investigated in the present study for $\xi^2 = 1$. Results were obtained via the improved MF theory (both one- and two-loop levels) and SCOZA (for different values of α—see text); lines as indicated in the legend. In addition, a line connecting the respective critical points is drawn.

$$D(\rho, u^C) = -\rho \frac{\partial^2 u^C}{\partial \rho^2}. \tag{33}$$

Once the PDE (32) is solved, further thermodynamic quantities (notably the pressure and the chemical potential) follow via standard thermodynamic relations.[15,36]

While previous applications of SCOZA were rather dedicated to the determination of the coexistence curves and to a reliable location of the critical point within reasonable accuracy, we rather focus in the present contribution on a *quantitative* description of the critical properties. This means that we have to approach the critical point very closely: introducing $\tau = (T - T_c)/T_c$, we need accurate and reliable data down to $\tau \sim 10^{-10}$ or even less. Compared to previous SCOZA applications this requires a considerable increase in the numerical accuracy. We have realized this goal by suitable modifications of the code and by increasing the default numerical accuracy to fourfold (extended) precision. Taking these measures is, in particular, indispensable for small α and ξ^2 values, where the Coulomb and Yukawa potentials at contact differ by many orders of magnitude. Of course this increase in numerical accuracy is accompanied by a considerable increase in computational effort.

C. Comparison between the theoretical approaches

In Fig. 1 we show the phase diagram of the system for $\xi^2 = 1$. We display results obtained from the improved MF theory both on the one- and on the two-loop level. We show also SCOZA results, varying the index α from 1.8 down to 0.01, which—within numerical accuracy—is already very close to the Kac limit. We observe that in this limit the SCOZA data really "converge" to the results obtained within the improved MF theories. A more detailed analysis shows that for $\alpha = 0.01$, the SCOZA data coincide with the results obtained on the one-loop level, while there is a slight difference with respect to the two-loop level. This outcome is valid for any value of ξ. Although a formal proof may be difficult, the limit $\alpha \to 0$ of SCOZA will reproduce the exact
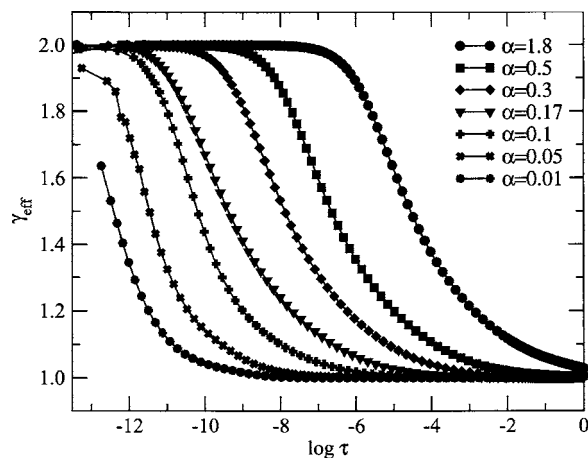

FIG. 2. (Effective) critical exponent γ as a function of τ (for the definition see text) of the system investigated in the present study for $\xi^2 = 0.16$ as obtained from SCOZA for different values of α, lined symbols as indicated in the legend.

MF result for $h^Y(r)$ and $c^Y(r)$, while $h^C(r)$ and $c^C(r)$ are solutions of the MSA. The one-loop theory is precisely built with these ingredients and should coincide with SCOZA as $\alpha \to 0$. The MF2L theory improves $h^C(r)$ and $c^C(r)$ for all ξ, although for $\xi \to 0$ the improvement is minor (cf. Sec. V). Comparison with simulation data will show that the two-loop level indeed represents an improvement. An even more elaborate version of the two-loop version of the improved MF theory that requires the pair distribution function to vanish inside the core will certainly lead to an even better agreement with simulations.

In Fig. 2 we show results obtained for the effective critical exponent γ_{eff} as a function of τ, obtained from SCOZA for $\xi^2 = 0.16$ and for a sequence of α values; α varies from 1.8 down to 0.01. γ characterizes the divergence of the compressibility as one approaches the critical point from *above*, i.e., $\chi_T \sim \tau^{-\gamma}$. The effective exponent γ_{eff} is obtained by differentiating the logarithm of χ_T with respect to the logarithm of τ along the critical isochore. While in the MF universality class γ is 1, its SCOZA value[16] (mean spherical) is 2.

For $\alpha > 0.2$, γ_{eff} varies with decreasing τ as found in the computations of this exponent by SCOZA performed for systems with an Ising 3D critical behavior.[37] For $\alpha < 0.1$ this variation of γ_{eff} is strongly modified. We observe that γ_{eff} keeps a MF value in the temperature domain $10^{-7} < \tau < 10^{-4}$, before crossover to the mean spherical exponent value takes place. The region of crossover shrinks drastically as α is lowered. At $\alpha = 0.01$ the MF behavior is found up to $\tau = 10^{-9}$, indicating that the critical behavior is likely to be MF over the *entire* τ range at $\alpha = 0$ as expected in the Kac limit (cf. Introduction and Sec. III A).

IV. SIMULATIONS

A. Methods

A detailed test of the validity of the theoretical approaches has been made by comparison with GCMC simulations. The GCMC simulations are performed on a hypersphere using the approach, detailed in Refs. 19 and 20, where the system of charged spheres is viewed as a single compo-

nent fluid of charged bihard spheres constrained to move at the surface of a four dimensional sphere. The practical implementation of this method, which is particularly adapted and efficient for simulating Coulomb systems of size $N < 10\,000$, can be found in Ref. 40.

Sampling of configuration space of the system is made according to the GC probability distribution,

$$p(N, R^N, \xi, \mu, T, V)$$
$$= \frac{V^N \exp\{\beta[\mu N - U_{\mathrm{RPM}}(R^N) - U_{\mathrm{MF}}(N, V, \xi)]\}}{N! \Lambda^{3N} \Xi(T, V, \mu, \xi)}. \quad (34)$$

Here Ξ is the grand canonical partition function[20] and R^N indicates the positions of the N charged spheres (or charged bihard spheres); $U_{\mathrm{RPM}}(R^N)$ is the energy of the RPM comprising Coulomb and hard core interactions. The term $U_{\mathrm{MF}}(N, V, \xi) = -aq^2\xi^2 N^2$ (with $a = 2\pi/V$) is the MF contribution to the internal energy as explicited in Sec. III A.

For each value of ξ, we determine the critical point and, in its vicinity, the coexistence line of the GL transition. The location of the latter is obtained from the histograms,

$$H(N, u, \xi, \mu, T, V)$$
$$= C \int dR^N \delta[u - U_{\mathrm{RPM}}(R^N)] p(N, R^N, \xi, \mu, T, V), \quad (35)$$

where C is a constant of normalization. By integration of $H(N, u, \xi, \mu, T, V)$ over u, one obtains the histogram $h(N, \xi, \mu, T, V)$ which shows, in the vicinity of the GL coexistence line, two peaks located at $N = N_g$ and N_l, respectively, and corresponding approximately to the densities ρ_g and ρ_l of the gas and the liquid.

At given T and ξ, the values of $\mu_e(L)$ (L characteristic size of the system defined as $V^{1/3}$) corresponding to GL equilibrium are affected by finite size effects. Therefore the estimates of $\mu_e(L)$ are made for increasingly large volumes and are then extrapolated to the thermodynamic limit. Several procedures are possible to define for a finite volume V the states of GL coexistence: First one can determine $\mu_e(L)$ such that the two peaks in $h(N, \xi, \mu, T, V)$ have equal area.[38] This procedure, however, does not allow, at fixed V, a very precise location of the critical point as in its vicinity the two peaks of $h(N, \xi, \mu, T, V)$ tend to merge. A second method to locate, at fixed V, phase equilibrium as well as critical temperatures and densities has been proposed by Wilding and Bruce.[6] It relies on the use of histograms of the variable $\mathcal{M} = \rho - s(u - aq^2\xi^2 N^2)/V$,

$$p(\mathcal{M}, \xi, \mu, T, V)$$
$$= \int du \sum_N \delta(\mathcal{M} - \rho + s(u - aq^2\xi^2 N^2)/V)$$
$$\times H(N, u, \xi, \mu, T, V). \quad (36)$$

For an appropriate choice of the parameter s, $\mathcal{M}$ is such that at GL equilibrium and near the critical point the distribution $p(\mathcal{M}, \xi, \mu, T, V)$ satisfies the symmetry relation,

$$p(\mathcal{M} - \langle \mathcal{M} \rangle, \xi, \mu, T, V) = p(-\mathcal{M} + \langle \mathcal{M} \rangle, \xi, \mu, T, V), \quad (37)$$

expected for the order parameter that characterizes phase transitions of the Ising 3D or the MF universality class. Validity of the field mixing approach[6,39] implies that, at the GL phase equilibrium, the histogram $h(N, \xi, \mu, T, V)$ corresponding to the symmetrized distribution $p(\mathcal{M}, \xi, \mu, T, V)$ has two peaks of equal area.

A third possibility is to apply an unbiased finite size scaling method presented by Fisher and co-workers.[8,41]

If one defines $x = \langle \delta \mathcal{M} \rangle / \langle \delta \mathcal{M}^2 \rangle^{1/2}$ with $\delta \mathcal{M} = \mathcal{M} - \langle \mathcal{M} \rangle$, the critical temperature $T_c(L)$ is obtained by determining the values μ, T, and s, which enable to fit $p(x, \xi, \mu, T, V) \equiv p(x)$ to the critical distribution $p_c(x)$ of the order parameter of a system of known universality class. For example $p_c(x)$ can be the distribution of magnetization of the Ising 3D model or that of the order parameter of a lattice spin model of the mean field universality class. For the Ising 3D model $p_c(x)$ is known accurately from MC simulations[42] and exactly for the MF universality class (see below). The values $T_c(L)$ obtained for increasingly large volumes V can then be extrapolated to obtain $T_c(\infty)$.

From the histograms $p(x)$ obtained at fixed volume the moments $\langle \delta \mathcal{M}^2 \rangle$ and $\langle \delta \mathcal{M}^4 \rangle$ can be calculated and from these the fourth order cumulant, $Q_L(\beta) = \langle \delta \mathcal{M}^2 \rangle^2 / \langle \delta \mathcal{M}^4 \rangle$, which in the vicinity of $T_c(\infty) = 1/\beta_c$, has the form[43]

$$Q_L(\beta) = Q^* + a_1(\beta - \beta_c)L^{y_\tau} + a_2(\beta - \beta_c)^2 L^{2y_\tau}$$
$$+ a_3(\beta - \beta_c)^3 L^{3y_\tau} + \cdots + b_1 L^{y_i} + \cdots. \quad (38)$$

Q^* and the exponents y_τ and y_i are characteristics of the universality class of the system and can be determined, together with β_c, by a fit of the $Q_L(\beta)$ obtained for different system sizes.

For the MF universality class $p_c(x) = A \exp(-ax^4)$ with $A = [\Gamma(3/4)]^2 2^{1/4}/\pi^{3/2}$, $a = \frac{1}{2}[\Gamma(3/4)]^4/\pi^2$, $Q^* = 2[\Gamma(3/4)]^4/\pi^2 = 0.456\,947$, $y_\tau = d/2 = 1.5$, and $y_i = -d/2 = -1.5$, where d is the dimensionality of the system.[44,45] As is well known the MF exponents do not satisfy hyperscaling. In comparison, for the Ising 3D universality class, $Q^* = 0.629$, $y_\tau = 1.59$, and $y_i = -0.83$.[46]

B. Results

Simulations have been performed for the values $\xi^2 = 100$, 11.11, 1.0, 0.1, 0.05, and 0.02 and volumes $V = 1000$, 4000, 8000, and 16 000. For each pair of ξ^2 and V of the order of $(5-10) \times 10^9$ MC trial moves were sampled. At volume $V = 16\,000$, even for such a large number of configurations the statistical error remained large so that the determination of phase equilibrium and the location of the critical point was based solely on the smaller volumes. Furthermore, a reweighting procedure allowed to extend the results obtained at the ξ values listed above to neighboring values of ξ.

An approximate location of the GL transition inferred from the appearance of two peaks in the histograms $h(N, \xi, \mu, T, V)$ indicates that (T_c, ρ_c) varies from approximately (113, 0.25) at $\xi^2 = 100$ to (0.075, 0.11) at $\xi^2 = 0.02$. From these values we can conclude that for the range of ξ

TABLE I. Variation of the critical temperatures and densities with ξ^2: T_c^Q—critical temperature obtained from the intersection of the cumulants $Q_L(\beta)$; $T_c(L)$ and $\rho_c(L)$—fit of simulation data at $V=8000$ to the universal MF distribution; T_c^S and ρ_c^S—SCOZA (with $\alpha=0.01$); $T_c^{(2)}$ and $\rho_c^{(2)}$—MFL2. For statistical error see text.

ξ^2	T_c^Q	$T_c(L)$	$\rho_c(L)$	T_c^S	ρ_c^S	$T_c^{(2)}$	$\rho_c^{(2)}$
100.0	113.5	113.4	0.250	113.2	0.249	113.2	0.249
100/9	$\cdots$	12.62	0.251	12.60	0.249	12.60	0.249
1.0	$\cdots$	1.172	0.242	1.163	0.243	1.173	0.243
0.10	0.1596	0.1599	0.190	0.148	0.176	0.1604	0.193
0.05	0.1054	0.1062	0.151	0.0972	0.0959	0.1066	0.135
0.02	0.0742	0.0748	0.111	0.0825	0.0225	0.0850	0.032

values considered, the critical temperature of our model is markedly higher than the critical temperature of the RPM ($\xi^2=0$), i.e., $T_c^{\mathrm{RPM}} \sim 0.049$.[23]

From the fact that T_c is larger than T_c^{RPM}, and the analyticity of the free energy at the critical point established in Sec. III A, it follows that the critical behavior of our model belongs to the MF universality class. In particular, the critical exponents in Eq. (38) giving $Q_L(\beta)$ near the critical point are MF-like and in the procedure of Bruce and Wilding,[6] $p(x)$ has to be adjusted to the distribution $p_c(x)$ of a model with MF criticality.

In Table I we summarize the critical temperatures $T_c(L)$ obtained at $V=8000$ by fitting $p(x)$ to the distribution $p_c(x)$ corresponding to the MF universality class and T_c^Q estimated from the fit of $Q_L(\beta)$ calculated for the volumes $V=1000$, 4000, and 8000 at the six values of ξ^2 considered in the simulations. The fits of $Q_L(\beta)$ are realized with five free parameters and Q^*, y_τ, and y_i fixed at their MF values [cf. Eq. (38)]. $Q_L(\beta)$ was calculated, for each volume, along the coexistence line by the procedure outlined above, and, for $T > T_c(L)$, for values of μ and s such that $p(x)$ remained symmetric with respect to $x=0$. For each volume, 8–12 values of $Q_L(\beta)$ were determined in the neighborhood of $T_c(L)$, i.e., $\approx \pm 3\%$ from $T_c(L)$. These temperatures T_c^Q are in good agreement with values for $T_c(L)$ obtained at $V=8000$ (cf. Table I). In the table $\rho_c(L)$ denotes the average density of the thermodynamic states at $\mu_c(L)$ and $T_c(L)$.

The considered values of ξ^2 were too different to allow reweighting in the whole range of parameters $\xi^2 > 0.1$. However, it was possible to combine histograms obtained at $\xi^2 = 0.05$ and 0.1, on one hand, and those at $\xi^2 = 0.02$ and 0.05, on the other. Furthermore, the results at $\xi^2 = 0.10$ could be reweighted up to 0.13, and those at $\xi^2 = 0.02$ to 0.01. However, combination of the $H(N, u, \xi, \mu, T, V)$ was possible only at volume $V=1000$ due to insufficient overlap of the energies at the larger volumes.

Figures 3 and 4 show the variation of $T_c(L)$ and $\rho_c(L)$ as a function of ξ^2 between $\xi^2 = 0.01$ and 0.13 for $V=1000$. GL coexistence curves are presented in Figs. 5–8 for $\xi^2 = 0.02$, 0.05, 1.0, and 11.11 and the three volumes $V=1000$, 4000, and 8000. The error in $T_c(L)$ is of the order of $\sim 0.3\%$–0.1% depending on the amount of sampling of the histograms $h(N, \xi, \mu, T, V)$. $T_c(L)$ decreases weakly ($\sim 1\%$) when V varies from 1000 to 8000 and differs from T_c^Q by about 1%. From these results it is concluded that in the range
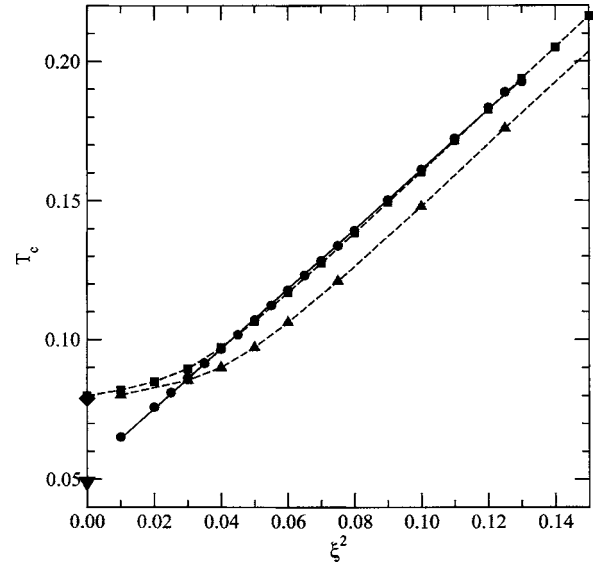

FIG. 3. Variation of the critical temperature T_c with strength ξ^2 of the Kac potential: MF2L—squares and dashed line, SCOZA—triangles up and dashed line, and solid circles—MC simulations for $V=1000$ (see text). The solid line is a linear fit of the simulation data. Diamond and triangle down indicate the critical temperatures of the RPM ($\xi^2=0$) obtained by the MSA approximation (Ref. 26) and simulation (Refs. 23 and 25), respectively.

$0.01 < \xi^2 < 0.13$, the values of $T_c(L)$ obtained by reweighting for $V=1000$ provide an estimate of T_c^Q or $T_c(L)$ at $V=8000$ with an uncertainty of the order of $\sim 1\%$ (cf. Table II).

The variation of the critical density with volume is small (cf. Table II), of the order of the statistical error on $h(N, \xi, \mu_c(L), T_c(L), V)$, estimated to be $\sim 0.5\%$–1.0% depending on sampling in the simulations. A second estimate of ρ_c, denoted $\rho_c^d(L)$, is based on the rule of rectilinear diameter, i.e., $\rho_c^d(L) = [\rho_g(T, L) + \rho_l(T, L)]/2$ valid at a MF critical point for T close to T_c. The values of $\rho_c^d(L)$ given in Table II for the different values of ξ and V were obtained by retaining only the coexistence densities $\rho_g(T, L)$ and $\rho_l(T, L)$, which were
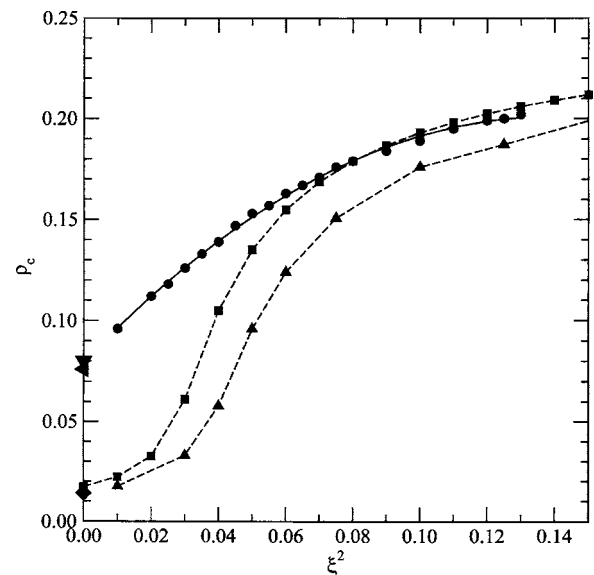

FIG. 4. Same as Fig. 3 but for the critical density ρ_c. The MC results for the RPM are from Ref. 23 (triangle down) and Ref. 25 (triangle left), respectively.
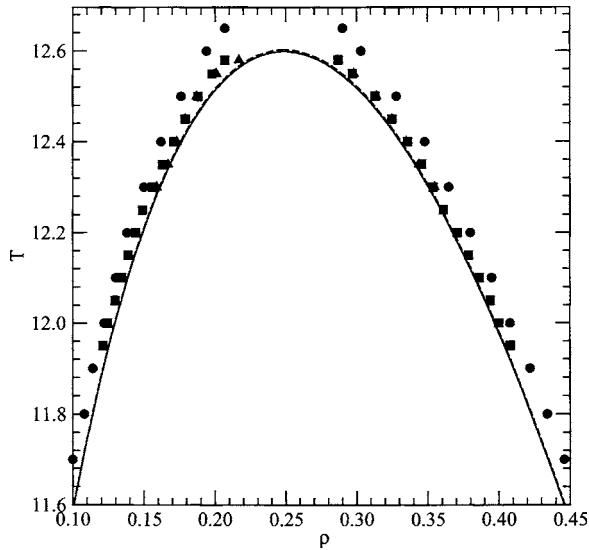
FIG. 5. Comparison between simulation and theoretical estimates for the coexistence curve at $\xi^2 = 100/9$ in the vicinity of the critical point. The symbols represent MC results for the different volumes: $V = 1000$ (circles), $V = 4000$ (squares), and $V = 8000$ (triangles); MF2L (dashed line); and SCOZA (full line).

FIG. 7. Coexistence curve at $\xi^2 = 0.05$ in the vicinity of the critical point. The symbols represent MC results for the different volumes: $V = 1000$ (circles), $V = 4000$ (squares), and $V = 8000$ (triangles); and MF2L (dashed line). The inset shows SCOZA (full line) and the one-loop approximation (diamonds).

closest to the critical point at $T_c(L)$ and $\rho_c(L)$. The coexistence densities $\rho_g(T, L)$ and $\rho_l(T, L)$ correspond to the two maxima of $h(N, \xi, \mu, T, V)$ whose associated distribution $p(x)$ is symmetric (see above). The uncertainty of the location of the maxima of $h(N, \xi, \mu, T, V)$ increases when T approaches $T_c(L)$ so that the error on $\rho_c^d(L)$ is of the order of $\sim 2\%$. The result for $\rho_c^d(L)$ is somewhat lower than $\rho_c(L)$ though compatible within the combined error estimates.

As mentioned previously in the literature,[7] agreement of $p(x)$ with a $p_c(x)$ characteristic of a universality class is necessary but not sufficient to make unambiguous conclusions about the universality class of a model system when studied by simulation. This uncertainty is illustrated for $\xi^2 = 0.02$ and $V = 8000$ in Fig. 9, which shows excellent fits of both the $p_c(x)$'s corresponding to the Ising 3D and MF universality classes.

As stated above, $T_c(L)$ can be estimated from a fit of $p(x)$ to the MF $p_c(x)$ distribution and T_c^Q from the fits of
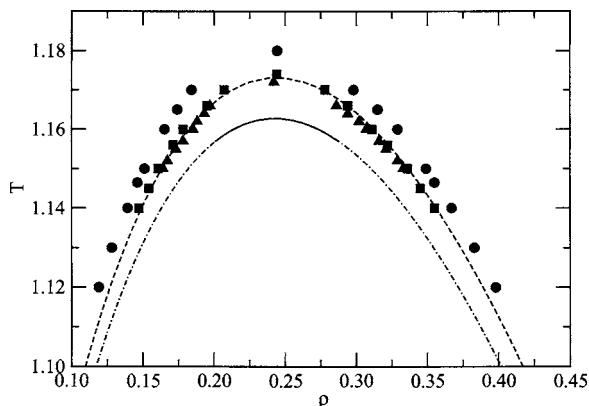
$Q_L(\beta)$ realized with five free parameters and Q^*, y_τ, and y_i fixed at their MF values. The uncertainties on $T_c(L)$ and T_c^Q, equal to 1–2%, are due to the statistical and systematic errors on $p(x)$ and $Q_L(\beta)$ which are of the order of 1%–2%. It corresponds to simulations of $(5-10) \times 10^9$ MC trial moves for each volume and ξ value. It results mainly, as already discussed in Ref. 23 for the case of the RPM critical point, from the low densities at which the GL critical point occurs in our model for $\xi^2 < 0.2$. However, such an uncertainty on the MC estimates of $Q_L(\beta)$ and the limited range of considered volumes in the simulations does not allow a direct and precise estimate of Q^*, y_τ, and y_i as it should result from the fit of $Q_L(\beta)$ with the eight free parameters present in Eq.

FIG. 6. Coexistence curve at $\xi^2 = 1$ in the vicinity of the critical point. The symbols represent MC results for the different volumes: $V = 1000$ (circles), $V = 4000$ (squares), and $V = 8000$ (triangles); MF2L (dashed line); SCOZA (full line); and one-loop approximation (dash-dotted line).
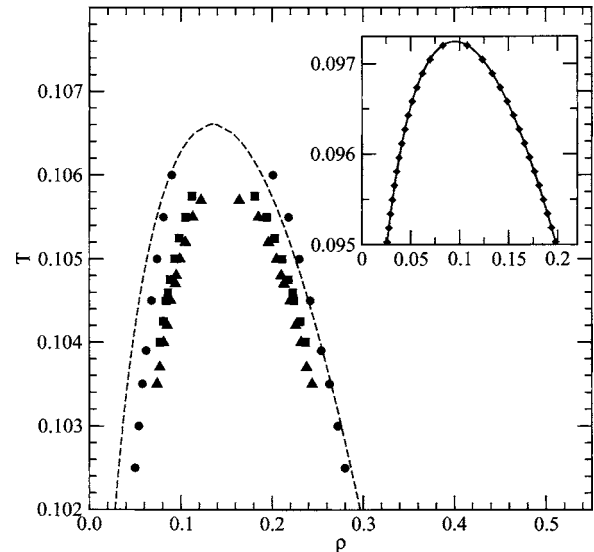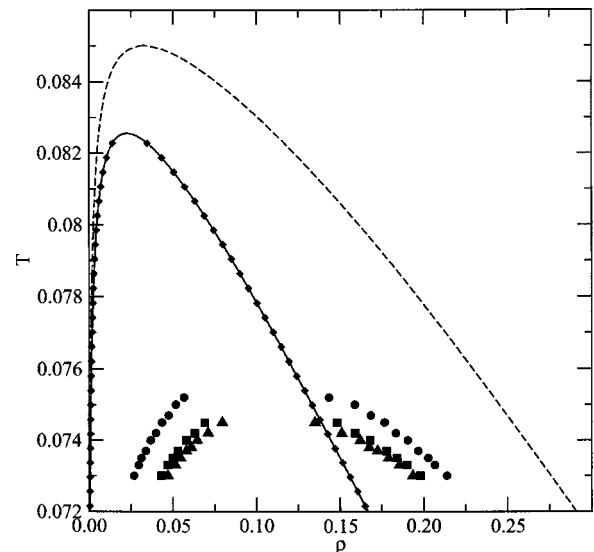

FIG. 8. Coexistence curve at $\xi^2 = 0.02$ in the vicinity of the critical point. The symbols represent MC results for the different volumes: $V = 1000$ (circles), $V = 4000$ (squares), and $V = 8000$ (triangles); MF2L (dashed line); SCOZA (full line); and one-loop approximation (diamonds).

TABLE II. Variation of the critical temperatures and densities with system size and ξ^2: $T_c(L)$ and $\rho_c(L)$—fit of simulation data at volume V to the universal MF distribution; $\rho_c^d(L)$—from rule of rectilinear diameter (see text). For statistical error see text.

ξ^2	V	$T_c(L)$	$\rho_c(L)$	$\rho_c^d(L)$
0.020	1000	0.075 95	0.112	0.102
0.020	4000	0.075 06	0.111	0.108
0.020	8000	0.074 77	0.111	0.108
0.050	1000	0.107 09	0.153	0.146
0.050	4000	0.106 20	0.151	0.147
0.050	8000	0.106 25	0.151	0.143
0.100	1000	0.161 25	0.189	0.183
0.100	4000	0.160 15	0.189	0.186
0.100	8000	0.159 93	0.190	0.187
1.0	1000	1.181	0.244	0.244
1.0	4000	1.174	0.244	0.243
1.0	8000	1.172	0.242	0.239
100.0	1000	114.0	0.250	0.249
100.0	4000	113.5	0.245	0.248
100.0	8000	113.4	0.247	0.246

FIG. 10. Fourth order cumulant $Q_L(\beta)$ as a function of inverse temperature β at volumes $V=1000$ (solid circles), 4000 (squares), and 8000 (triangles) at $\xi^2=0.02$. The lines are fits of the simulation data using 8 free parameters, in Eq. (38).

(38). In spite of the fact that the agreement of such fits with MC data is quite good (examples are presented in Figs. 10 and 11), the uncertainties on Q^*, y_τ, and y_i are of the order of 20%–30%.

V. COMPARISON: THEORIES VERSUS COMPUTER SIMULATIONS

While the results obtained of the two theories and the simulation data have already been discussed in the respective subsections, we focus in the following on a direct comparison between the theoretical and the simulation data.

To this end we go back to Table I where we have collected critical data (i.e., T_c and ρ_c) for different values of ξ^2

as obtained from the GCMC simulations, the improved MF theory, and SCOZA; in the latter case we have chosen $\alpha = 0.01$, i.e., a value that has turned out to be sufficiently small to make the potential $v^Y(r)$ Kac type. From these data we can conclude that both theories are able to reproduce the critical temperatures and critical densities for large and intermediate values of $\xi^2 \gtrsim 1$ very accurately. In the range of ξ^2 values, 0.06–1, the MF2L approximation remains quantitative, while SCOZA differs from the simulation results by $\approx 10\%$ for the critical temperature and $\approx 30\%$ for the critical density. Below $\xi^2 \sim 0.06$ the RPM contribution to the potential becomes dominant and we find, not surprisingly, that the theoretical data start to differ from the simulation results; in both theo-
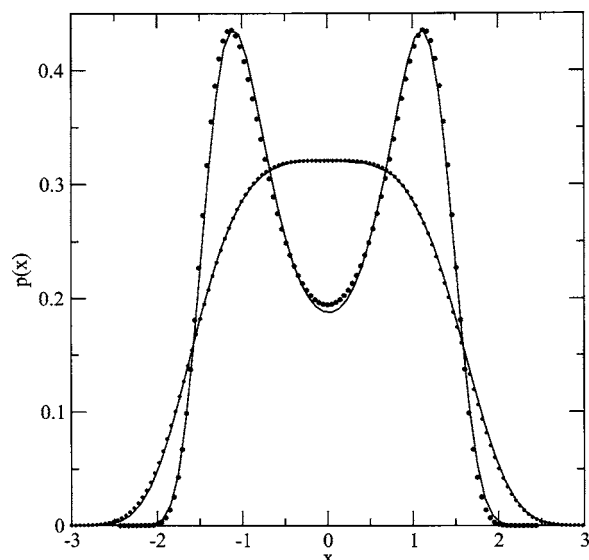

FIG. 9. Matching of $p_c(x)$ Ising 3D ($T=0.073\,85$, $\mu=-9.7953$, and $s=-1.03$) (two peaks) and $p_c(x)$ MF ($T=0.074\,77$, $\mu=-9.6901$, and $s=-0.98$) at $\xi^2=0.02$ and $V=8000$.
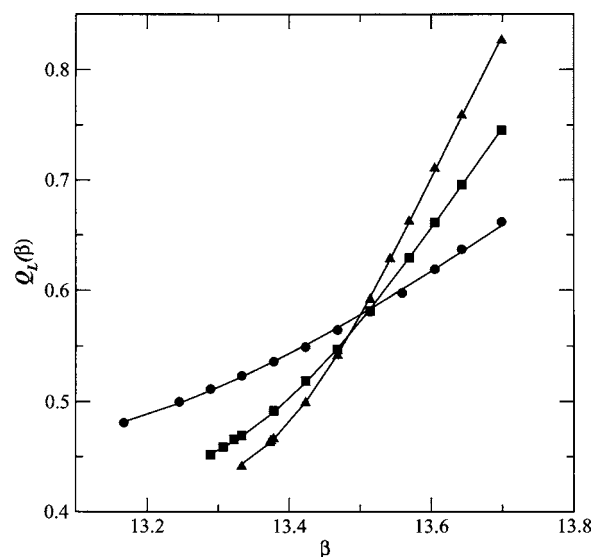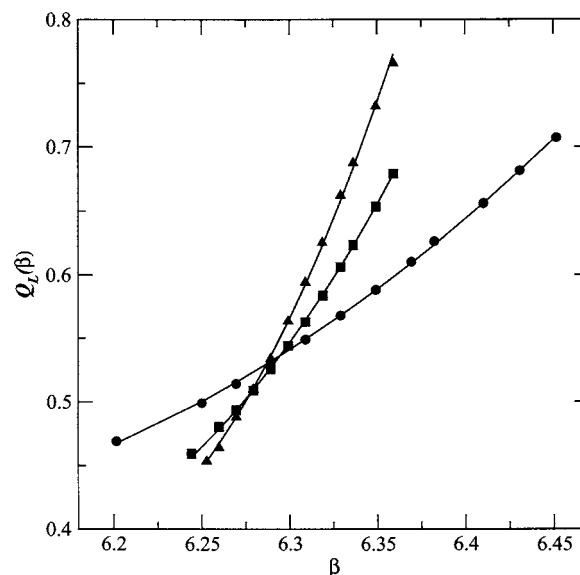

FIG. 11. Fourth order cumulant $Q_L(\beta)$ as a function of inverse temperature β at volumes $V=1000$ (solid circles), 4000 (squares), and 8000 (triangles) at $\xi^2=0.1$. The lines are fits of the simulation data using 8 free parameters, in Eq. (38).

ries, critical temperature and density tend to the MSA values of the RPM for $\xi^2=0$ whose failure to reproduce the simulation data for the RPM is well documented.[17] As pointed out above, SCOZA identifies with the one-loop MF theory for all ξ^2 as $\alpha \rightarrow 0$.

The coexistence curves in the vicinity of the critical point obtained from theory and simulation are compared in Figs. 5–8 for selected values of ξ^2. The convergence of the coexistence curves with system volume can be appreciated from these figures; the results obtained for volume $V=8000$ appear to be close to the infinite system limit. The MF2L approximation for the coexistence curve agrees well with simulation data for $\xi^2 > 0.1$ but deteriorates when approaching the RPM limit where the critical temperature is overestimated and the critical density is underestimated. One should note, however, that even at $\xi^2=0.02$ the critical temperature differs from the MC result by only 10%. The MF2L approximation is a definite improvement over either the one-loop approximation or SCOZA and could still be improved by requiring the pair distribution function to vanish inside the core at the two-loop level.

As noted above, SCOZA provides data that are in a less satisfactory agreement with simulation data than those of the improved MF theory. Despite this deficiency, SCOZA was able to provide useful information about the critical behavior of the system: having nonclassical critical exponents we have been able to trace the crossover from a MF to a non-MF behavior, as we approach the Kac limit (see Fig. 2), verifying that the system displays MF criticality for $\alpha=0$.

VI. CONCLUSION AND OUTLOOK

We have investigated the critical behavior of a system where the interaction is a linear combination of two potentials, each of them having a well-defined critical behavior, viz., Ising 3D or MF. Taking the RPM for the first contribution and a Kac-type potential for the latter one, we could vary via a parameter ξ^2 the weight of the respective contributions. Our investigations have been carried out with GCMC simulations and two theoretical approaches, i.e., SCOZA and the improved MF theory. The theoretical argument of Sec. III shows that the MF behavior at the critical point is expected for all $\xi^2 \neq 0$.

We have given a detailed account how the simulations and the theoretical approaches perform in the critical region. We showed that the three theories considered in this work (SCOZA, MF1L, and MF2L) provide a quantitative determination of the location of the critical point of the considered model. In addition the SCOZA results provide strong evidence when $\alpha \rightarrow 0$ for a MF value of the effective γ_{eff} up to a distance 10^{-9} to the critical temperature before crossover to the mean spherical value of 2 occurs.

The location of the GL critical point (based on the MF universality class) and the coexistence lines are obtained from simulation within a numerical accuracy of $\sim 1\% - 2\%$ with a slight variation with the volume V. For our model we find excellent agreement between the theoretical approaches and computer simulations for ξ^2 values down to ~ 1; the improved MF theory, MF2L, performs in an excellent way

even down to $\xi^2 \sim 0.05$. Only for very small values of ξ^2, i.e., close to the pure RPM, simulation data and theoretical results start to deviate.

We highlight the ambiguity arising when determining critical temperatures by fitting universal critical point order distribution functions by showing that for the present system almost equally good fits are obtained for both the universal Ising 3D and MF distributions.

Finally, by referring to the theoretical developments presented in Sec. III A, we can remark that the critical temperature is obtained by requiring that the second derivative of $\mathcal{L}(\beta, \nu, \rho)$ with respect to the density vanishes, which yields

$$\beta_c \partial^2 f_{\text{RPM}}(\rho, \beta)/\partial \rho^2 \sim \chi_T^{-1} = 2\pi\beta_c q^2 \xi^2, \qquad (39)$$

where χ_T denotes the isothermal compressibility of the RPM. Arguing that for small ξ^2 $\chi_T \sim |T_c - T_c^{\text{RPM}}|^\gamma$, where γ is the critical exponent of the compressibility of the RPM (or, more generally, that of the system with potential v_{IS}), it is concluded that

$$T_c - T_c^{\text{RPM}} \sim \xi^{2/\gamma}. \qquad (40)$$

This relation provides a means to evaluate the exponent γ. By simulation this turns out to be practical only for large systems ($V \gtrsim 20\,000$) which are necessary to accurately sample the density distribution function in the very low density gas phase of the RPM near the critical point as stressed already in Sec. III A.

[1] C. Caccamo, Phys. Rep. **274**, 1 (1996).
[2] A. Parola and L. Reatto, Adv. Phys. **44**, 211 (1995).
[3] A. Parola and L. Reatto, Phys. Rev. Lett. **53**, 2417 (1984); Phys. Rev. A **31**, 3309 (1985); for a more recent overview see also A. Reiner and G. Kahl, Phys. Rev. E **65**, 046701 (2002); A. Reiner and G. Kahl, J. Chem. Phys. **117**, 4925 (2002); D. Pini, M. Tau, A. Parola, and L. Reatto, Phys. Rev. E **67**, 046116 (2003).
[4] J.-P. Hansen and I. McDonald, *Theory of Simple Liquids*, 3rd ed. (Cambridge University Press, Cambridge, 2006).
[5] G. Stell, Phys. Rev. **184**, 135 (1969).
[6] N. B. Wilding and A. D. Bruce, J. Phys.: Condens. Matter **4**, 3087 (1992).
[7] Y. C. Kim and M. E. Fisher, J. Phys. Chem. B **108**, 6750 (2004).
[8] Y. C. Kim, M. E. Fisher, and E. Luijten, Phys. Rev. Lett. **91**, 065701 (2003).
[9] M. Kac, G. E. Uhlenbeck, and P. C. Hemmer, J. Math. Phys. **4**, 216 (1963).
[10] J. L. Lebowitz and O. Penrose, J. Math. Phys. **7**, 98 (1966).
[11] J. S. Høye and G. Stell, J. Chem. Phys. **67**, 439 (1977).
[12] J. S. Høye and G. Stell, Mol. Phys. **52**, 1071 (1984).
[13] D. Pini, G. Stell, and N. B. Wilding, Mol. Phys. **95**, 483 (1998).
[14] G. Kahl, E. Schöll-Paschinger, and A. Lang, Monatsch. Chem. **132**, 1413 (2001).
[15] E. Schöll-Paschinger and G. Kahl, Europhys. Lett. **63**, 538 (2003).
[16] J. S. Høye, D. Pini, and G. Stell, Physica A **279**, 213 (2000).
[17] J. M. Caillol, Mol. Phys. **103**, 1271 (2005); e-print cond-mat/0409455.
[18] J.-M. Caillol, Mol. Phys. **104**, 1931 (2006); e-print cond-mat/0602205.
[19] J. M. Caillol and D. Levesque, J. Chem. Phys. **94**, 597 (1992).

[20] J. M. Caillol, J. Chem. Phys. **99**, 8953 (1993).

[21] A. M. Ferrenberg and R. H. Swendsen, Phys. Rev. Lett. **61**, 2635 (1988); **63**, 1195 (1989).

[22] N. B. Wilding, Phys. Rev. E **52**, 602 (1995).

[23] J. M. Caillol, D. Levesque, and J.-J. Weis, J. Chem. Phys. **116**, 10794 (2002).

[24] E. Luijten, M. E. Fisher, and A. Z. Panagiotopoulos, Phys. Rev. Lett. **88**, 185701 (2002).

[25] A. Panagiotopulos, J. Chem. Phys. **116**, 3007 (2002).

[26] G. Stell, J. Stat. Phys. **78**, 197 (1995).

[27] Y. Levin and M. E. Fisher, Physica A **225**, 164 (1996).

[28] O. V. Patsahan, Condens. Matter Phys. **7**, 35 (2004).

[29] N. Goldenfeld, *Lectures on Phase Transitions and the Renormalization Group* (Addison-Wesley, New York, 1992).

[30] N. F. Carnahan and K. Starling, J. Chem. Phys. **51**, 635 (1969).

[31] T. Kristóf, D. Boda, J. Liszi, D. Henderson, and E. Carlson, Mol. Phys. **101**, 1611 (2003).

[32] E. Schöll-Paschinger and G. Kahl, J. Chem. Phys. **118**, 7414 (2003).

[33] E. Waisman, Mol. Phys. **25**, 45 (1973).

[34] F. H. Stillinger and R. Lovett, J. Chem. Phys. **48**, 3858 (1968).

[35] E. Waisman and J. L. Lebowitz, J. Chem. Phys. **56**, 3093 (1972).

[36] E. Schöll-Paschinger, Ph.D. thesis, Institut für Theoretische Physik, TU Wien, 2002.

[37] D. Pini, G. Stell, and N. B. Wilding, Mol. Phys. **95**, 483 (1998).

[38] C. Borgs and R. Kotecky, J. Stat. Phys. **60**, 79 (1990).

[39] J. J. Rehr and N. D. Mermin, Phys. Rev. A **8**, 472 (1973).

[40] J. M. Caillol, D. Levesque, and J.-J. Weis, J. Chem. Phys. **107**, 1565 (1997).

[41] Y. C. Kim and M. E. Fisher, Comput. Phys. Commun. **169**, 295 (2005).

[42] M. M. Tsypin and H. W. J. Blöte, Phys. Rev. E **62**, 73 (2000).

[43] H. W. J. Blöte, E. Luijten, and J. R. Heringa, J. Phys. A **28**, 6289 (1995).

[44] E. Luijten, *Interaction Range, Universality and Upper Critical Dimension* (Delft University Press, Delft, 1997).

[45] E. Luijten and H. W. J. Blöte, Phys. Rev. Lett. **76**, 1557 (1996).

[46] Y. Deng and H. W. J. Blöte, Phys. Rev. E **68**, 036125 (2003).

[47] L. D. Landau and E. M. Lifshitz, *Statistical Physics* (Pergamon, London, 1959).